

# Proposal on the Calculation of the Ionisation-Cluster Size Distribution

## (I). The Model and Its Simulation Methodology

(B. Heide, Karlsruhe Institute of Technology (KIT), Institute for Nuclear Waste Disposal (INE),  
Bernd.Heide@kit.edu)

### Abstract

A statistical model for the calculation of the ionisation-cluster size distribution in nanodosimetry is proposed. It is based on a canonical ensemble and derives from the well-known nuclear droplet model. The model especially can be applied to the scenario "low energy primaries (< 100 eV) moving in nanovolumes (in the order of a few nanometers)" – a scenario to which trajectory models should not be used. The focus of this work is on presenting the model and demonstrating its feasibility.

### 1. Introduction

In the macroscopic range, i.e. for volumes with a size of millimetres or more, the absorbed dose ( $D_{\text{abs}}$ ) and the linear energy transfer are good measures for the action of ionising radiation inside soft matter. However, although the model quantity  $D_{\text{abs}}$  is a point quantity, it is often inadequate for the microscopic ( $\mu\text{m}$ ) length scale. This is because  $D_{\text{abs}}$  refers to the average absorbed energy. But deviations from the average value, which can become relatively large for volumes in the range of micrometres, are important since a single ionisation (i.e., energy deposition) can decompose a critical molecule and hence cause a serious radiation damage (cf. Ref.<sup>(1)</sup>). In microdosimetry,  $D_{\text{abs}}$  is therefore replaced by the specific energy, which is a stochastic quantity in contrary to  $D_{\text{abs}}$  which is a statistical one. Likewise, in microdosimetry, the linear energy transfer, which refers to a mean (!) energy lost and can be understood in the general sense as "force", is replaced by a stochastic quantity: the lineal energy.

If one now considers even smaller volumes, i.e. nanometric volumes, one finds that the number of ion pairs generated in a gas detector is no longer proportional to the deposited energy. In nanodosimetry, the quantities "specific energy" and "lineal energy" are therefore no longer investigated. Instead, the focus is only on the ionisations generated in the target. The collectivity of ionisations generated in the target is denoted as "ionisation cluster (ic)"; their count is referred to as "size (s)". Nanometric volumes are well suited for analysing biological damage at the level of deoxyribonucleic acid (DNA).

There are several models for describing biological damage once a cell was exposed to ionising radiation. The reader is referred to Refs.<sup>(2-11)</sup>, for instance. Besides the model of W. Friedland et al.<sup>(3)</sup>, S. A. Ngcezu and H. Rabus<sup>(7)</sup>, B. Grosswendt<sup>(8,9)</sup> as well as the model of F. Villegas et al.<sup>(10)</sup>, the models already start from an initial ionisation (energy deposition) aggregation or even from DNA single-strand breaks (SSBs) and double-strand ones (DSBs). However, it is in general not explicitly stated how the initial ionisation aggregation is transformed into clusters of ionisations and clusters of DNA fragments, respectively. On the other hand, the models that deal with clustering contain at least one free parameter, i.e. a parameter for which there may be a relatively large margin of error (such as the cluster distance in Ref.<sup>(10)</sup>; it causes preselected ionisation-cluster sizes to some extent). In addition, all of the above models have one major disadvantage in common: their theoretical descriptions are based on classical trajectories. And this generally makes little sense for low-energy particles that move in nanovolumes as the spatial extension of their wave packet is usually larger than the target volume itself! For example, if an initial electron is expected to move in a cube with a dimension of 2 nm and has an energy of (almost exactly) 100 eV and a well defined momentum (i.e. a relative uncertainty of 1%) then Heisenberg's uncertainty principle gives a spatial extension of the electron wave packet of about 12 nm (= 6 times the cube length) or more. An approximate illustration of this situation is shown in Figure 1. However, it is assumed that

the amount of ionisation interactions alone should not be affected by the Heisenberg uncertainty principle in contrast to the trajectories (see Ref.<sup>(12)</sup>).

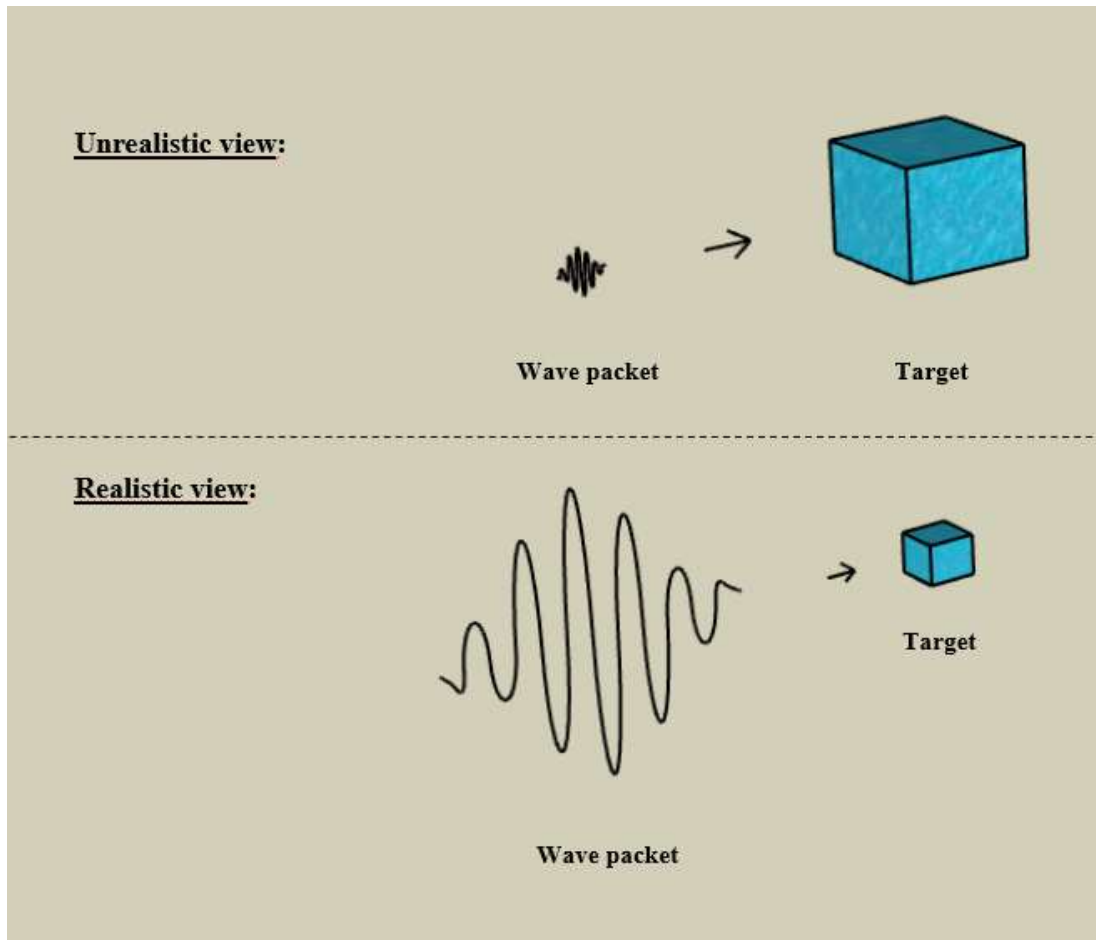


Figure 1: approximate illustration of the proportions between the wave packet and the cube-shaped target. Upper half: unrealistic view (classical). Lower half: realistic view (quantum mechanical).

In the following, we

(a) propose a ('semi-classical' in a sense) statistical model for the calculation of the ionisation-cluster size (**ics**) distribution in nanodosimetry which is detached from exact location information and uses as input only the total number of ionisations within a target volume, that can be determined by a Monte Carlo particle transport code (such as the program package Geant4-DNA (cf. Ref.<sup>(13, 14, 24-26)</sup>)) and hence has no free parameter, and

(b) depict its simulation methodology in detail.

The model is based on a canonical ensemble and derives from the well-known nuclear droplet model (cf. Ref.<sup>(19, 20)</sup>), which has already been applied successfully for the prediction of nuclear-cluster distributions. It can be applied in particular to a so-called "transition zone" for which the classical description using trajectories is no longer adequate and the quantum mechanical one is too time-consuming and/or complicated. The model especially can be seen as a refinement to B. Grosswendts model (s. Ref.<sup>(8, 9)</sup>) in the sense that the size of the ionisation clusters can be broken down into smaller ones.

The next section is about the model. Following on, its numerical realisation will be discussed in Section 3. As the model takes a new approach, a critical assessment of the present work is given in Section 4. And finally, a summary and outlook is given at the end in Section 5.

## 2. Model

Recall that the spatial extension of the wave packet usually is larger than the target volume for low energy (i.e.  $\leq 100$  eV) particles moving in nanometric volumes. So, the classical description, which is based on trajectories, has come to a limit. The appropriate description would have to be within the framework of quantum mechanics. The explicit calculations, however, would be too sophisticated and time consuming. The model that follows is an attempt to do it better than the classical description and quicker than the quantum mechanical one, although the latter would of course be best. The model is intended as an alternative proposal and still offers room for improvement. It is based on the following scenario and assumptions: starting point is a nanometric target volume made of liquid water (a DNA polymer could also be used instead of liquid water). The volume is irradiated with direct ionising (primary) particles which could have low energy in particular. Target and primary particles (including source) can be in a vacuum or embedded in a medium (e.g., air or water). The primary particles can be protons or electrons, for example; we will focus on electrons below. An illustration of this scenario is shown in Figure 2.

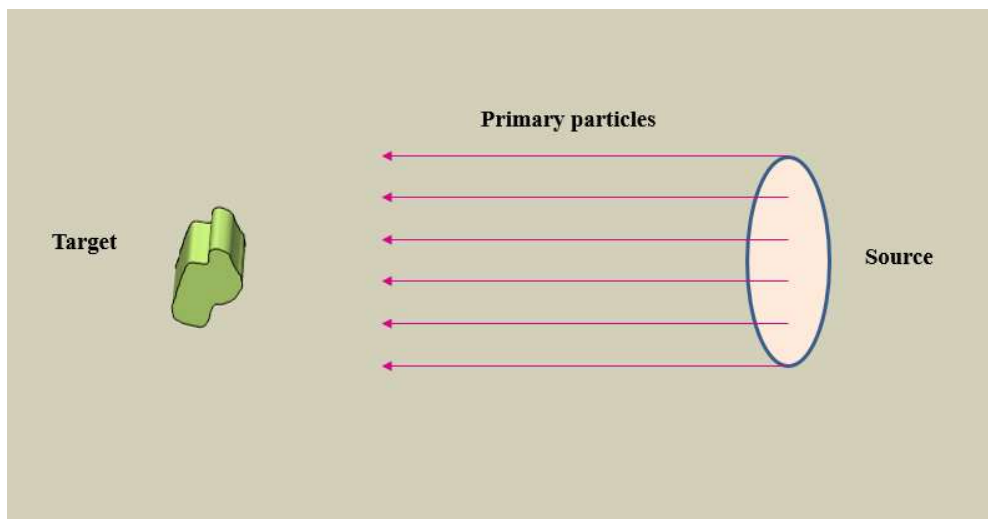


Figure 2: exemplary illustration of an underlying scenario. The target can be arbitrarily shaped. The primary particles are ionising. Without loss of generality, a plane-parallel, homogeneous source was drawn. Target, primary particles, and source can be embedded in a medium (e.g., air or water).

Ionisations may occur due to the interactions of the primary particles as well as secondary electrons (and higher-generation electrons, respectively) with the material. Furthermore, we assume that the ionisations and the subsequent ‘rearrangement processes’ in the target volume lead to an order-disorder phase transition, whereby the statistics dominate (due to the large number of degrees of freedom being involved) the dynamics (which become very complex at the phase transition; correlation length diverges) and the size of the individual clusters of ionisations present after these actions can be described by a stochastic distribution based on the free energy.

We base our statistical (ionisation-clustering) model, which is built on a canonical ensemble, on the following nomenclature:

- $n_t$ : total number of ionisations; it is in some sense equivalent to  $D_{\text{abs}}$ .
- $n_j$ : number of  $j$  interrelated ionisations. The following applies:  
 $j \in [1, \dots, k]$  and  $n_k \leq n_t$ . We call  $j$  interrelated ionisations an "ionisation cluster of size  $j$ ". Its probability of occurrence is determined via the free energy.
- $q(I)$ : number of partitions of  $I$  ( $I$  denotes a positiv integer), whereat a partition is a sequence of ionisation clusters
- $\vec{n}_t$ :  $t$ -dimensional partition vector,  $(n_1, n_2, \dots, n_t)^t$ , describing one of the  $q(n_t)$  partitions; it is in some respect equivalent to the lineal energy. Please note: a partition vector is not a "real" vector in terms of Euclidean geometry.
- $\{\vec{n}_t\}$ : set of all possible  $q(n_t)$   $t$ -dimensional partition vectors
- $M$ : ionisation-cluster multiplicity of a partition, i.e. number of ionisation clusters of a partition

$(n_t, M)$ : macrostate consisting of all microstates which refer to  $n_t$  ionisations and  $M$  ionisation clusters  
 $q(n_t|M)$ : number of partitions (microstates) of  $n_t$  with ionisation-cluster multiplicity  $M$ . Note:  $q(n_t|M)$  is not equal with the conventional partition sum in general.  
 $L$ : likelihood of a macrostate  
 $V$ : nanometric volume  
 $T$ : temperature  
 event: consists of a primary particle moving through  $V$   
 $F$ : free energy. The following shall apply:  $F(n_t, M)$  is the free energy which refers to macrostate  $(n_t, M)$ .  
 $\epsilon_0$ : vacuum permittivity  
 $k_B$ : Boltzmann constant

Clarification regarding partitions:

If there are  $n_t = 5$  ionisations, then, there are  $q(5) = 7$  partition vectors  $\vec{n}_{5,i}$  ( $i = 1, \dots, 7$ ).  
 This means,  $\{\vec{n}_5\} = \{ \vec{n}_{5,1} = (5, 0, 0, 0, 0)^t, \vec{n}_{5,2} = (3, 1, 0, 0, 0)^t, \vec{n}_{5,3} = (1, 2, 0, 0, 0)^t, \vec{n}_{5,4} = (2, 0, 1, 0, 0)^t, \vec{n}_{5,5} = (0, 1, 1, 0, 0)^t, \vec{n}_{5,6} = (1, 0, 0, 1, 0)^t, \vec{n}_{5,7} = (0, 0, 0, 0, 1)^t \}$ . The partition vector  $\vec{n}_{5,4}$  refers to two ionisation clusters of size 1 and to one ionisation cluster of size 3. There are  $q(5|3) = 2$  partition vectors with ionisation-cluster multiplicity  $M = 3$  (which belong to macrostate  $(5, 3)$ ):  $\vec{n}_{5,3}$  and  $\vec{n}_{5,4}$ .

The basic idea of the model is as follows. For all events do:

- calculate all possible partitions of the amount of ionisation interactions,
- calculate free energy  $F$  and temperature  $T$ ,
- choose a macrostate due to " $\exp\{-F((n_t, M), T, V)/T\}$ " and then select a microstate with equal probability.

### 3. Simulation Methodology

The methodology reads as follows in detail:

#### (1) Numerical calculation of $n_t$

To calculate the total number of ionisations,  $n_t$ , a scoring volume with shape of a cylinder is preconditioned (without loss of generality). The material inside the cylinder is DNA or DNA equivalent matter (which, for example, can be liquid water for the time being) as mentioned above. The numerical calculation is done using a classical particle transport code (like Geant4-DNA<sup>(13, 14, 24-26)</sup>, MDM<sup>(15)</sup>, or PARTRAC<sup>(16)</sup>; an overview of common classical particle transport codes can be found in Ref.<sup>(17)</sup>). We presume here that  $n_t$  will not much change for a quantum multiple-scattering calculation since ionising interactions are inelastic ones, i.e. we suppose a circumstantial validity of the trajectory method (cf. Ref.<sup>(12)</sup>).

#### (2) Computation of $\{\vec{n}_t\}$ and selection of $\vec{n}_t$

The number of partitions of  $n_t$  can become very large: if  $n_t = 10$ , then  $q(10) = 42$ , but if  $n_t = 100$ , then  $q(100) = 190569292$  (and  $q(1000) = 24061467864032622473692149727991$ ); s. Ref.<sup>(18)</sup>.

If the number of partitions is small, i.e. if, for example, all macrostates can be calculated within 2 hours cpu time, then we take into account all partition vectors and choose a macrostate and finally one partition vector as described in subsection (2.1) below.

If the number of partitions is not small, we propose to consider "biased" subsets of the multidimensional partition space (cf. Ref.<sup>(19)</sup>) and then apply the procedure of subsection (2.1).

#### (2.1) Calculation of likelihood $L$

To clarify the structure of the calculation of the likelihood  $L$ , we divide this section into two subsections, termed (2.1.1) and (2.1.1.1), where the subsection (2.1.1.1) has to be calculated before the

subsection (2.1.1). For the calculation of  $L$ , we assume that a macrostate  $(n_t, M)$  can be described within the canonical approximation, i.e. the likelihood of  $(n_t, M)$  is given by

$$L = c * \exp\{-F((n_t, M), T, V)/T\}, \quad (1)$$

where " $c$ " is a normalisation constant, " $F$ " is the free energy of the system being in macrostate  $(n_t, M)$  as well as in thermal equilibrium, and " $T$ " is the temperature. The nanometric target volume is designated with " $V$ ". Having choosen a macrostate  $(n_t, M)$ , one of its microstates, described by  $\vec{n}_t$ , is selected with equal probability then.

### (2.1.1) Calculation of free energy $F$

The free energy " $F$ " of a macrostate is assumed to be the sum of "translational" parts " $F_j^{tr,Z}$ " and "inner" parts " $n_j F_j^{in}$ ",

$$F((n_t, M), T, V) = \sum_{j=1}^{n_t} (F_j^{tr,Z} + n_j F_j^{in}), \quad (2)$$

with " $n_j$ " is the number of ionisation clusters of size " $j$ ". Each  $n_j$  contains the contributions of the corresponding microstates:

$$n_j = \sum_{k=1}^{q(n_t|M)} n_{j,k}, \quad (3)$$

where " $n_{j,k}$ " refers to the number of ionisation clusters of size " $j$ " of microstate " $k$ ", and " $q(n_t|M)$ " denotes the amount of microstates which belong to macrostate  $(n_t, M)$ .

For the explicit calculation of the translational part " $F_j^{tr,Z}$ " of the free energy, we assume that the ionisation clusters behave in the same way as particles of a Boltzmann gas, i.e. their spatial distribution is essentially uniform. We assume further that the ionisation clusters are within a cylindrical volume  $V$ . Furthermore, the Coulomb interaction is treated by means of the mean-field approximation.

Let  $\vec{x}$  contain the coordinates of all ionisation clusters. The canonical partition sum reads then,

$$Z(T, n_j, V) = \frac{\lambda_T^{-3n_j}}{n_j!} \int e^{-\beta V_m(\vec{x})} d^{3n_j} x. \quad (4)$$

The integration is over volume  $V$ . The abbreviation  $\lambda_T$  indicates the thermal de Broglie wavelength,

$$\lambda_T = \frac{h}{\sqrt{2\pi m k_B T}}, \quad (5)$$

where " $h$ " denotes Planck constant and " $m$ " is the mass of the ionisations clusters of size " $j$ ". The mass results from mass density and volume, and the volume from a radius " $\tilde{r}_k$ " (which computation is depicted when the calculation of " $F_j^{in}$ " is discussed [s. below]). The factor " $k_B$ " is the Boltzmann constant, and the thermodynamic beta reads,  $\beta = 1/(k_B T)$ . The term with respect to the mean-field potential, i.e. the Coulomb energy of the ionisation clusters in their own field, is denoted by  $V_m$ . It explicitly reads,

$$V_m = \frac{1}{4\pi\epsilon_0} \frac{3 e^2 j^2}{5 R}, \quad (6)$$

where " $\epsilon_0$ " is the vacuum permittivity, " $e$ " is the elementary charge, and " $R$ " is the radius of a sphere having the same volume as the target volume (the difference between the cylindrical and the spherical shape is neglected, which seems justified due to the small dimensions). It follows for the canonical partition sum after integration:

$$Z(T, n_j, V) = \frac{\lambda_T^{-3n_j}}{n_j!} V^{n_j} e^{-\beta V_m}. \quad (7)$$

Finally, we find for the translational part " $F_j^{tr,Z}$ ":

$$F_j^{tr,Z} = -k_B T \ln Z(T, n_j, V). \quad (8)$$

The term " $F_j^{in}$ " of the inner parts is obtained using a generalisation of the well-known nuclear droplet model. For the time being, we consider the Coulomb contribution only for the calculation of  $F_j^{in}$ . Starting point is the Coulomb energy  $E_j^C$  of " $j$ " charges which are homogeneously distributed within a sphere of radius " $\tilde{r}_k$ ":

$$E_j^C = \frac{1}{4\pi\epsilon_0} \frac{3}{5} \frac{e^2 j^2}{\tilde{r}_k}. \quad (9)$$

The radius " $\tilde{r}_k$ " is obtained as follows: first of all, we assume that a molecule has an admittedly somewhat inadequate cubic shape and the ions should touch each other. The error resulting from the inadequate shape of volume should be negligible due to the small dimension of the volume (similar as mentioned above). The same applies to further changes to the geometric shape further below. One side " $r_j$ " of the cube of an ionisations cluster of size " $j$ " is then given by,

$$r_j = (j V_{molecule})^{\frac{1}{3}}, \quad (10)$$

where  $V_{molecule}$  is the molecule volume. Next, we scale  $r_j$  such that the molecule density inside the cube of the ionisation clusters of size " $j$ " is equal to the molecule density " $\rho$ " of the target volume:

$$r_j \rightarrow r_k = k r_j, \quad (11)$$

with

$$k = (j^2 \rho V_{molecule})^{-\frac{1}{3}}. \quad (12)$$

Then the radius " $\tilde{r}_k$ " is calculated as

$$\tilde{r}_k = (3/(4\pi))^{\frac{1}{3}} r_k, \quad (13)$$

where the factor " $(3/(4\pi))^{\frac{1}{3}}$ " results from the conversion of the cubic volume into a spherical volume of the same size. We assume  $E_j^C$  to be (almost) not dependent on the temperature. Therefore, there is only one microstate which is associated with this energy. The respective entropy is hence zero. So, we can write

$$F_j^{in} = E_j^C. \quad (14)$$

### (2.1.1.1) Calculation of temperature T

The temperature T is obtained from the absorbed energy " $E_{abs}$ ", which is described by

$$E_{abs} = \frac{3 e^2 n_t^2}{20 \pi \epsilon_0 R} + \sum_{j=1}^{n_t} n_j [F_j(T, V) - T \left( \frac{\partial F_j(T, V)}{\partial T} \right)_V] - E_0. \quad (15)$$

The first term on the right hand side refers to the Coulomb energy of a homogeneously charged sphere of radius R. Then follows the internal energy. The term " $E_0$ " denotes the ground-state energy. We approximate  $E_0$  by the corresponding expression for an ideal gas,

$$E_0 = \frac{3}{2} n_t k_B T_{initial}, \quad (16)$$

where " $T_{initial}$ " denotes the initial temperature. The absorbed energy can be computed by one of the classical particle transport codes mentioned above (see subsection (1)); just as  $n_t$ . After a very tedious (albeit elementary) calculation, Equation (15) can finally be transformed in a simple but very long term for the temperature. This long term takes the form "absorbed energy multiplied by a factor minus an additional term". For the sake of simplicity, this long term is not specified. As an alternative to Eq. (15), one could also calculate the temperature using the Saha equation<sup>(21)</sup> or using the specific heat capacity<sup>(22)</sup> for the temperature increase.

### (3) Sorting ionisation clusters into a histogram

This is done as usual.

### (4) Repeating No 1 to 3 until end is reached

The end is determined by the total number of events.

## 4. Critical Assessment

The model described above is an attempt to overcome the limitations of clustering models – which are due to the low energy primaries moving in nanovolumes on the one hand and are manifested in a parameter such as the 'cluster distance' on the other that is selectable in certain limits only. In this respect,

it is intended in particular to offer an alternative to previous practice, in which classical models and software packages, respectively, are also applied to the case "low energy ( $< 100$  eV) primaries moving in nanovolumes (in the order of a few nanometers)". Furthermore, in contrast to previous cluster models, the model allows statements to be made about the thermodynamic state quantities entropy and free energy, respectively, and the temperature. In addition, the model could be tailored relatively easily to a grand-canonical ensemble or a micro-canonical one as well. The model therefore offers a relatively large potential of application. But beware! The basic concept was presented in Section 2 only. The model still provides ample scope for individual improvements, e.g. with regard to the parameterisation of the free energy and the temperature calculation. Therefore, the model necessarily still needs to be evaluated thoroughly and carefully. This is particularly important with regard to the assumption of the order-disorder phase transition – which may well be the most critical assumption of the model. A thoroughly and carefully done evaluation is subject of a forthcoming paper. For the time being, we will content ourselves with a discussion of initial simulations in which Geant4-DNA calculations were carried out largely without the actually necessary adjustment of the parameter values and the interaction cross-sections, and 100 events only were taken into account. Therefore, the following results should be understood as possible indications only.

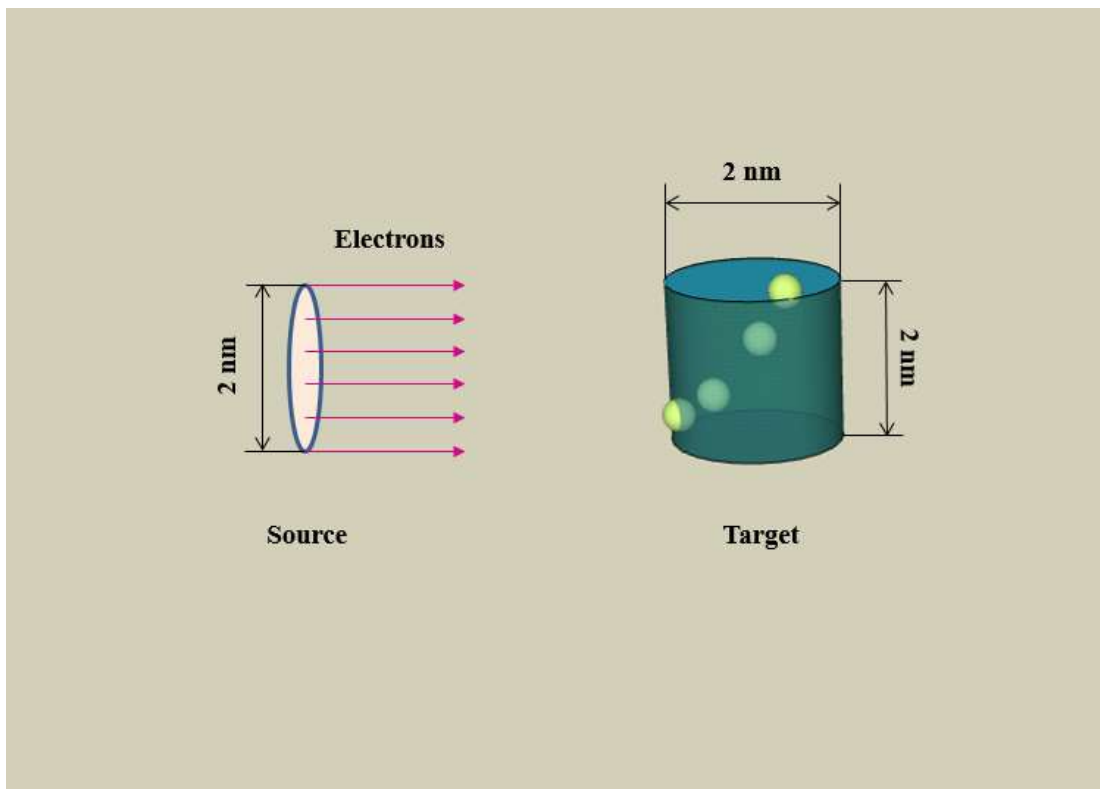


*Figure 3: a cylindrical target, made of liquid water, is irradiated with monoenergetic electrons emitted from a planar circular area (source). The target and the source are in vacuum. The small spheres symbolise some ionisation interactions that have taken place inside the target.*

In what follows, we refer to a scenario previously described by B. Grosswendt<sup>(9)</sup>, cf. Figure 3: monoenergetic electrons, having kinetic energies between 70 eV and 5 keV, are homogeneously emitted from a planar circular area with a diameter of 2 nm. Their direction is parallel to the surface normal. The electrons impinge on a cylinder with a diameter and height of 2 nm. The planar circular area is located such that the centre-line of the area is perpendicular to the cylinder's main axis and crosses the latter at half its height. Both the planar circular area and the cylinder are in vacuum. The cylinder consists of liquid water.

We calculated " $E_{\text{abs}}$ " using the program package Geant4-DNA<sup>(13, 14, 24-26)</sup>. The parameter " $n_t$ " was derived from the quantities  $F_1$ ,  $F_2$ , and  $F_3$  from Fig. 6 of Ref.<sup>(9)</sup>. The model itself was realised by means of an in-house object-oriented C++ program. The cpu time required for the computation of all macrostates was

in the region of seconds.

Below we compare our model with the models of B. Grosswendt<sup>(8, 9)</sup> and W. Friedland et al.<sup>(3)</sup>.

Grosswendt's model is essentially based on the following. Starting point is a primary particle that moves along a classical trajectory and either flies close to a cylindrical target, made of water, or hits it. The primary particle causes ionisations along its trajectory. Each vertex is a starting point of a secondary electron (and higher-generation electron, respectively) which can also cause ionisations inside the target. The probability "P<sub>1</sub>" that exactly 1 ionisation occurs in the target is described by

$$P_1 = \sum_{k=0}^{\infty} [f_1^{(1)}(d)]^{*k} \frac{\langle k \rangle^k}{k!} e^{-\langle k \rangle}. \quad (17)$$

And for the probability "F<sub>2</sub>" that ionisation clusters of size 2 or more are produced, we find

$$F_2 = \sum_{v=2}^{\infty} \sum_{k=0}^{\infty} [f_v^{(1)}(d)]^{*k} \frac{\langle k \rangle^k}{k!} e^{-\langle k \rangle}. \quad (18)$$

The term " $\langle k \rangle^k \exp(-\langle k \rangle) / k!$ " which appears in Eqs. (17) and (18), is the expression of the Poisson distribution. The term " $[f_v^{(1)}(d)]^{*k}$ " in Eq. (18) is the k-fold convolution of the probability " $f_v^{(1)}(d)$ " of cluster size "v" being formed in case of a single primary ionisation. This k-fold convolution represents the probability that, including the contribution by secondary electrons, a cluster size v is formed at distance "d" from the relevant particle path segment in case of k primary ionisations. In contrast to Eq. (18), the cluster size in Eq. (17) is set to "v = 1".

The model of W. Friedland et al., like Grosswendt's model, is also based on primary particles moving along classical trajectories and either fly close to the cylindrical target or hit it. And in particular, the target is also made of water. However, a very sophisticated DNA-target model is then used after the simulation of the particle tracks. The DNA-target model takes five levels of the B-DNA structure into account: nucleotides, DNA helices, nucleosomes, chromatin fiber structure, and chromatin fiber loops. The DNA-target model is superimposed upon the particle tracks. Finally, the yields of SSBs and DSBs are determined from spatial coincidences with strand atoms.

The model of W. Friedland et al. has so far been limited to single-event primary ionisations. It has two parameters – the energy necessary to create an SSB and the distance between two strand breaks that would be scored as a DSB – which are adapted to equate simulated and measured strand break yields.

Figure 4 shows the energy dependence of the yield of single-strand breaks "SSBs" and the probability of cluster-size one P<sub>1</sub>, respectively. The SSBs were calculated by W. Friedland et al.<sup>(2)</sup>, and the P<sub>1</sub> distribution either by B. Grosswendt<sup>(9)</sup> or with our model. Our purple P<sub>1</sub> distribution refers to temperature values which were calculated by means of Eq. (15). Our green P<sub>1</sub> distribution relates to temperature values that were obtained by using the specific heat capacity. Both our purple P<sub>1</sub> and green P<sub>1</sub> distribution refer to an initial temperature of 310.15 K. It can be inferred from Figure 4 that our model gives approximately the same results as the model of B. Grosswendt – regardless of the respective temperature calculation. All P<sub>1</sub> values (red, purple, green) are more or less close to the SSB values.



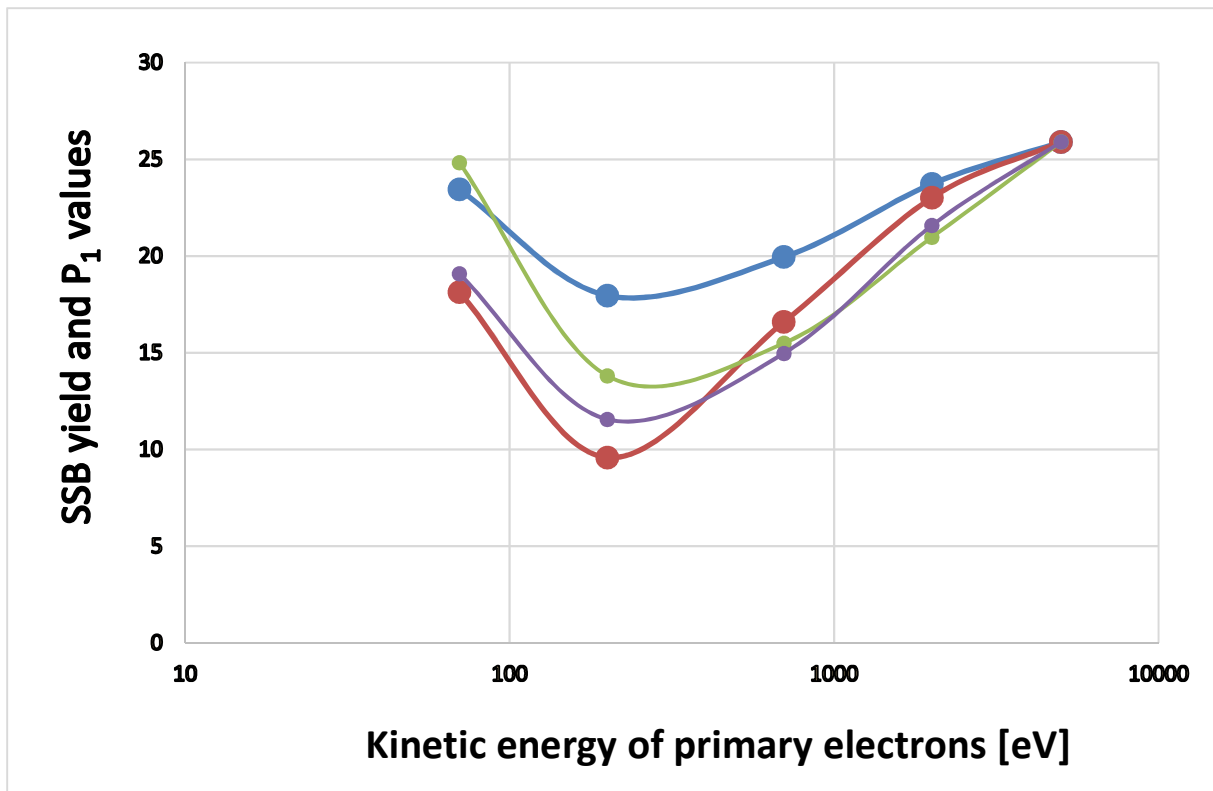


Figure 4: energy dependence of SSB yield in  $10^{-11} \text{ Gy}^{-1} \text{ Da}^{-1}$  (blue) as well as  $P_1$  distributions (red, purple, green). The data points refer to 70 eV, 200 eV, 700 eV, 2000 eV, and 5000 eV (abscissa). The SSB yield was calculated by W. Friedland et al.<sup>(3)</sup>, the red  $P_1$  distribution was computed by B. Grosswendt<sup>(9)</sup>. All data were taken from B. Grosswendt<sup>(9)</sup>. The purple and green  $P_1$  values were calculated by our model. The  $P_1$  values were scaled with the energy absorbed (B. Grosswendt) or with the mean No of ionisations (our model) for each data point. All  $P_1$  values were normalised to the SSB value at 5000 eV. See text for further explanation.

This behaviour changes regarding to the DSB values and  $F_2$  values, respectively. Figure 5 shows the energy dependence of the yield of double-strand breaks "DSBs" and of the  $F_2$  values. Analogue to the  $P_1$  values, our purple  $F_2$  distribution refers to temperature values which were calculated by means of Eq. (15), whereas our green  $F_2$  distribution relates to temperature values that were obtained by using the specific heat capacity. Both our purple  $F_2$  and green  $F_2$  distribution refer to an initial temperature of 310.15 K. It can be seen from Figure 5 that both of our  $F_2$  distributions match better with the DSB values than the  $F_2$  distribution of B. Grosswendt. In particular, the purple  $F_2$  curve is very similar to the DSB values. This result strengthens our belief that our model could be a refinement of B. Grosswendt's model. Both our results from Figure 4 and from Figure 5 are similar to the results of W. Friedland et al. as well as the ones of B. Grosswendt. So our model should not be so unreasonable, all things considered. However, our results in Figures 4 and 5 are subject to major uncertainties. The relative error is likely to be in the range between 30% and 40%. Please also note that information has been lost due to the normalisation of the data. Much more calculations need to be carried out for a proper validation! We would like to point out once again that the results are only to be understood as possible indications.

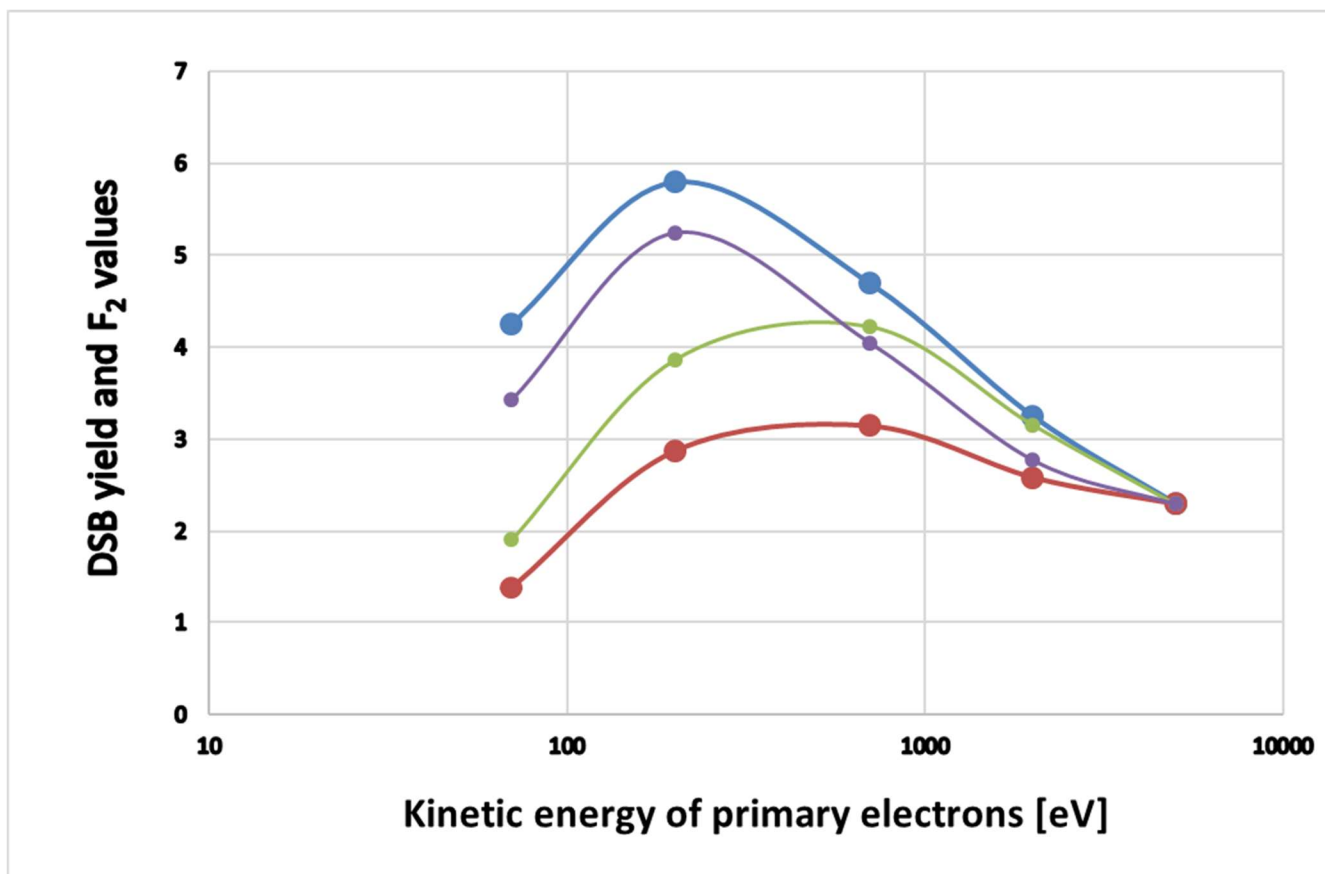


Figure 5: energy dependence of DSB yield in  $10^{-11} \text{Gy}^{-1} \text{Da}^{-1}$  (blue) as well as  $F_2$  distributions (red, purple, green). The data points refer to 70 eV, 200 eV, 700 eV, 2000 eV, and 5000 eV (abscissa). The DSB yield was calculated by W. Friedland et al.<sup>(3)</sup>, the red  $F_2$  distribution was computed by B. Grosswendt<sup>(9)</sup>. All data were taken from B. Grosswendt<sup>(9)</sup>. The purple and green  $F_2$  values were calculated by our model. The  $F_2$  values were scaled with the energy absorbed (B. Grosswendt) or with the mean No of ionisations (our model) for each data point. All  $F_2$  values were normalised to the DSB value at 5000 eV. See text for further explanation.

## 5. Summary and Outlook

A proposal on the calculation of the ionisation-cluster size distribution was depicted. The proposal is essentially based on the well-known nuclear droplet model<sup>(19, 20)</sup> and can be seen as a refinement to Bernd Grosswendts model<sup>(8, 9)</sup>. A first rough simulation with large uncertainties showed that our model in general led to similar results as the ones of B. Großwendt<sup>(9)</sup> as well as the ones of W. Friedland et al.<sup>(3)</sup>, and in particular resulted in a cluster-size distribution function  $F_2$  being more similar to the yield of double-strand breaks in the DNA, calculated by W. Friedland et al., than the one calculated by B. Grosswendt.

Our primary results strengthen our belief that our model should not be so unreasonable, all things considered. In contrast to previous models, our model allows statements about thermodynamic state quantities and it can be applied to the scenario "low energy primaries (< 100 eV) moving in nanovolumes (in the order of a few nanometers)" – a scenario to which trajectory models should not be used. However, much more work need to be carried out for a proper validation! This applies in particular for the parameterization of the free energy and the temperature calculation as well as for the assumed order-disorder phase transition. The labour-intensive work that still needs to be done is subject of a forthcoming paper. (A comparison with algorithms for DNA clustering into radiation-induced foci, cf.

Ref.<sup>(23)</sup>, also seems worthwhile.) The focus of this work was on presenting the model and demonstrating its feasibility.

## Acknowledgement

The author gratefully acknowledges the support of the NUSAFE programme.

## References

1. Rossi, H. H. and Zaider, M., *Microdosimetry and Its Applications*, Springer, Berlin (1996).
2. Cordoni, F., Missiaggia, M., Attili, A., Welford, S. M., Scifoni, E., and La Tessa, C., *Generalized stochastic microdosimetric model: The main formulation*, Phys. Rev. E 103, 012412 (2021).
3. Friedland, W., Jacob, P., Paretzke, H. G., and Stork, T., *Monte Carlo Simulation of the Production of Short DNA Fragments by Low-Linear Energy Transfer Radiation Using Higher-Order DNA Models*, Radiation Research 150, pp. 170 – 182 (1998).
4. Besserer, J. and Schneider, U., *A track-event theory of cell survival*, Z. Med. Phys. 25, 168 (2015).
5. Besserer, J. and Schneider, U., *Track-event theory of cell survival with second-order repair*, Radiat. Environ. Biophys. 54, 167 (2015).
6. Schneider, U., Vasi, F., Schmidli, K., and Besserer, J., *A model of radiation action based on nanodosimetry and the application to ultra-soft X-rays*, Radiat. Environ. Biophys. 59, 439 (2020).
7. Ngcezu, S. A. and Rabus, H., *Investigation into the foundations of the track-event theory of cell survival and the radiation action model based on nanodosimetry*, Radiat. Environ. Biophys. (2021).
8. Grosswendt, B., *NANODOSIMETRY, FROM RADIATION PHYSICS TO RADIATION BIOLOGY*, Radiation Protection Dosimetry, Vol. 115, pp. 1 – 9 (2005).
9. Grosswendt, B., *RECENT ADVANCES OF NANODOSIMETRY*, Radiation Protection Dosimetry, Vol. 110, pp. 789 – 799 (2004).  
The model goes back to: De Nardo, L., Colautti, P., Conte, V., Baek, W. Y., Grosswendt, B., and Torielli, G., *Ionization-cluster distributions of  $\alpha$ -particles in nanometric volumes of propane: measurement and calculation*, Radiat. Environ. Biophys. 41, 235–256 (2002).
10. Villegas, F., Bäckström, G., Tilly, N., and Ahnesjö, A., *Energy deposition clustering as a functional radiation quality descriptor for modeling relative biological effectiveness*, Med. Phys. 43 (12) (2016).
11. Garty, G., Schulte, R., Shchemelinin, S., Leloup, C., Assaf, G., Breskin, A., Chechik, R., Bashkirov, V., Milligan, J., and Grosswendt, B., *A nanodosimetric model of radiation-induced clustered DNA damage yields*, Med. Phys. 55, 761–781 (2010).
12. Liljequist, D. and Nikjoo, H., *On the validity of trajectory methods for calculating the transport of very low energy ( $< 1$  keV) electrons in liquids and amorphous media*, Radiation Physics and Chemistry 99, pp. 45 – 52 (2014).
13. Incerti, S., Baldacchino, G., Bernal, M., Capra, R., Champion, C., Francis, Z., Guatelli, S., Guèye, P., Mantero, A., Mascialino, B., et al., *The Geant4-DNA project*, Int. J. Model. Simul. Sci. Comput. 1, pp. 157 – 178 (2010).
14. Bernal, M. A., Bordage, M. C., Brown, J. M. C., Davidková, M., Delage, E., El Bitar, Z., Enger, S. A., Francis, Z., Guatelli, S., Ivanchenko, V. N., et al., *Track structure*

- modeling in liquid water: A review of the Geant4-DNA very low energy extension of the Geant4 Monte Carlo simulation toolkit*, Phys. Med. 31, pp. 861 – 874 (2015).
15. Poignant, F., Ipatov, A., Chakchir, O., Lartaud, P.-J., Testa, É., Gervais, B., and Beuve, M., *Theoretical derivation and benchmarking of cross sections for low-energy electron transport in gold*, Eur. Phys. J. Plus 135: 358 (2020).
  16. Paretzke, H. G., Turner, J. E., Hamm, R. N., Wright, H. A., Ritchie, R. H., *Calculated yields and fluctuations for electron degradation in liquid water and water vapor*, J. Chem. Phys. 84, pp. 3182 – 3188 (1986).
  17. Li, W. B., Belchior, A., Beuve, M., Chen, Y. Z., Di Maria, S., Friedland, W., Gervais, B., Heide, B., Hocine, N., Ipatov, A., Klapproth, A. P., Li, C. Y., Li, J. L., Multhoff, G., Poignant, F., Qiu, R., Rabus, H., Rudek, B., Schuemann, J., Stangl, S., Testa, E., Villagrasa, C., Xie, W. Z., and Zhang, Y. B., *Intercomparison of Dose Enhancement Ratio and Secondary Electron Spectra for Gold Nanoparticles Irradiated by X-rays Calculated Using Multiple Monte Carlo Simulation Codes*, Physica Medica 69, pp. 147-163 (2020). And corrigendum:  
Li, W. B., Beuve, M., Di Maria, S., Friedland, W., Heide, B., Klapproth, A. P., Li, C. Y., Poignant, F., Rabus, H., Rudek, B., Schuemann, J., and Villagrasa, C., *Corrigendum to "Intercomparison of Dose Enhancement Ratio and Secondary Electron Spectra for Gold Nanoparticles Irradiated by X-rays Calculated Using Multiple Monte Carlo Simulation Codes" [Phys. Med. 69 (2020), pp. 147-163]*, Physica Medica 80, pp. 383–388 (2020).
  18. Bruinier, J. H. and Ono, K., *Algebraic formulas for the coefficients of half-integral weight harmonic weak Maass forms*, arXiv:1104.1182 [math.NT], <https://doi.org/10.48550/arXiv.1104.1182> (accessed on 21 March 2024).
  19. Bondorf, J. P., Botvina, A. S., Iljinov, A. S., Mishustin, I. N., and Sneppen, K., *STATISTICAL MULTIFRAGMENTATION OF NUCLEI*, Physics Reports 257 pp. 133 – 221 (1995).
  20. Bondorf, J. P., Donangelo, R., Mishustin, I. N., Pethick, C. J., Schulz, H., and Sneppen, K., *STATISTICAL MULTIFRAGMENTATION OF NUCLEI, (I). Formulation of the model*, Nuclear Physics A443, pp. 321 – 347 (1985).
  21. Chen, Francis F., *Introduction to Plasma Physics and Controlled Fusion*, Springer International Publishing Switzerland, ISBN 978-3-319-22308-7 (2018).
  22. [https://phys.libretexts.org/Bookshelves/University\\_Physics/Physics\\_\(Boundless\)/13%3A\\_Heat\\_and\\_Heat\\_Transfer](https://phys.libretexts.org/Bookshelves/University_Physics/Physics_(Boundless)/13%3A_Heat_and_Heat_Transfer) (accessed on 25 September 2024).
  23. Poignant, F., Pariset, E., Plante, I., Ponomarev, A. L., Evain, T., Viger, L., Slaba, T. C., Blattnig, S. R., and Costes, S. V., *DNA break clustering as a predictor of cell death across various radiation qualities: influence of cell size, cell asymmetry, and beam orientation*, Integrative Biology, 16, zya015 (2024), <https://doi.org/10.1093/intbio/zya015> (accessed on 30 September 2024).
  24. Tran, H. N., Archer, J., Baldacchino, G., Brown, J. M. C., Chappuis, F., Cirrone, G. A. P., Desorgher, L., Dominguez, N., Fattori, S., Guatelli, S., Ivantchenko, V., Méndez, J.-R., Nieminen, P., Perrot, Y., Sakata, D., Santin, G., Shin, W.-G., Villagrasa, C., Zein, S., Incerti, S., *Review of chemical models and applications in Geant4-DNA: Report from the ESA BioRad III Project*, Med. Phys. 51, 5873–5889 (2024).
  25. Incerti, S., Kyriakou, I., Bernal, M. A., Bordage, M. C., Francis, Z., Guatelli, S., Ivantchenko, V., Karamitros, M., Lampe, N., Lee, S. B., Meylan, S., Min, C. H., Shin, W. G., Nieminen, P., Sakata, D., Tang, N., Villagrasa, C., Tran, H., Brown, J. M. C., *Geant4-DNA example applications for track structure simulations in liquid water: a report from the Geant4-DNA Project*, Med. Phys. 45, e722–e739 (2018).
  26. Incerti, S., Ivantchenko, A., Karamitros, M., Mantero, A., Moretto, P., Tran, H. N., Mascialino, B., Champion, C., Ivantchenko, V. N., Bernal, M. A., Francis, Z., Villagrasa,

C., Baldacchino, G., Guèye, P., Capra, R., Nieminen, P., Zacharatou, C., *Comparison of Geant4 very low energy cross section models with experimental data in water*, Med. Phys. 37, 4692–4708 (2010).